European Journal of Soil Science

European Journal of Soil Science, May 2017, **68**, 270–280 doi: 10.1111/ejss.12425

Evolution of loess-derived soil along a climatic toposequence in the Qilian Mountains, NE Tibetan Plateau

F. Yang[a,c], L. M. Huang[b,c], D. G. Rossiter[a,d], F. Yang[a,c], R. M. Yang[a,c] & G. L. Zhang[a,c]

[a]*State Key Laboratory of Soil and Sustainable Agriculture, Institute of Soil Science, Chinese Academy of Sciences, NO. 71 East Beijing Road, Xuanwu District, Nanjing 210008, China,* [b]*Key Laboratory of Ecosystem Network Observation and Modeling, Institute of Geographic Sciences and Natural Resources Research, Chinese Academy of Sciences, No. 11(A), Datun Road, Chaoyang District, Beijing 100101, China,* [c]*University of the Chinese Academy of Sciences, No.19(A) Yuquan Road, Shijingshan District, Beijing 100049, China, and* [d]*School of Integrative Plant Sciences, Section of Soil and Crop Sciences, Cornell University, Ithaca NY 14853, USA*

Summary

Holocene loess has been recognized as the primary source of the silty topsoil in the northeast Qinghai-Tibetan Plateau. The processes through which these uniform loess sediments develop into diverse types of soil remain unclear. In this research, we examined 23 loess-derived soil samples from the Qilian Mountains with varying amounts of pedogenic modification. Soil particle-size distribution and non-calcareous mineralogy were changed only slightly because of the weak intensity of chemical weathering. Accumulation of soil organic carbon (SOC) and leaching of carbonate were both identified as predominant pedogenic responses to soil forming processes. Principal component analysis and structural analysis revealed the strong correlations between soil carbon (SOC and carbonate) and several soil properties related to soil functions. Accretion of SOC effectively decreased soil bulk density ($R^2 = 0.81$) and increased cation exchange capacity ($R^2 = 0.96$), soil water retention at saturation ($R^2 = 0.77$), field capacity ($R^2 = 0.49$) and wilting point ($R^2 = 0.56$). These results indicate that soil ecological functions are strengthened during pedogenic modification of such loess sediments. Soil C/N ratio was constant at small SOC contents, but after reaching a threshold of approximately 35 g kg^{-1} SOC, soil C/N increased linearly with SOC. This indicates a change from a carbon-limited loess ecosystem in arid regions to a nitrogen-limited one in alpine settings. This research suggests that loess sequences within environmental gradients offer great potential as natural experiments to explore intrinsic soil behaviour and ecosystem evolution because the effect of parent material is well constrained.

Highlights

- We examined pedogenic modifications of loess with uniform origin from contrasting environments.
- Accumulation of SOC and depletion of carbonate coincide during pedogenesis of loess-derived soil.
- Pedogenesis underpins functional evolution of loess-derived soil across the Qilian Mountains.
- Loess sequences provide ideal natural experiments to study soil and ecosystem evolution.

Introduction

The Qilian Mountains commonly have a silty surface soil layer that has been derived from loess deposited since the early Holocene (Küster *et al.*, 2006; Kaiser *et al.*, 2007; Nottebaum *et al.*, 2015). These silt-textured loess sediments are typically carbonate rich and organic poor in origin. However, once deposited on the land surface, they undergo varying degrees of pedogenic modification in response to the contrasting environments (Liu, 1985). For example, in the northern foreland of the Qilian Mountains (Hexi Corridor), the soil is dry for most of the year and shows little pedogenic modification of the primary loess, whereas in an alpine setting the soil usually accumulates a large amount of organic carbon because of the low temperature and the soil's water regime (Küster *et al.*, 2006; Yang *et al.*, 2014).

There is a lack of research on the pedogenic processes that lead to the diversity of soil derived from primary loess in the Qilian Mountains or other mountains of the Tibetan Plateau. In contrast, many pedogenic studies have been carried out on loess-covered plains or plateau regions (e.g. the Eurasian steppe and central plain of the USA). In these studies, environmental

Correspondence: G. L. Zhang. E-mail: glzhang@issas.ac.cn

Received 12 September 2016; revised version accepted 7 March 2017

gradients were often identified over a large spatial extent, along which some soil processes, such as accumulation of soil organic carbon (SOC), leaching of carbonate and illuviation of clay, were studied quantitatively (e.g. Jenny, 1941; Walker & Everett, 1991; Klopfenstein *et al*., 2015). In the Qilian Mountains, however, it is difficult to establish a well-defined climatic or topographic soil sequence because of the considerable soil spatial heterogeneity and the lack of precise meteorological data. The complex terrain and variable climate make it difficult to determine the pedogenic responses to any particular soil forming factor.

Soil organic carbon and carbonate have been reported to correlate well with climatic factors in loess ecosystems (Liu, 1985; Schaetzl & Anderson, 2005; Klopfenstein *et al*., 2015); therefore, we assumed that they could be used as indicators of climate conditions and pedogenic intensities. Furthermore, SOC and carbonate are two fundamental attributes that affect many soil properties, including pH, cation exchange capacity (CEC), bulk density and soil water retention, which largely determine soil ecological functions (Walker & Everett, 1991; Meyer *et al*., 2008). It has been reported that SOC and carbonate vary considerably across the Qilian Mountains (Liu *et al*., 2012; Yang *et al*., 2014, 2015). Nevertheless, the way that soil ecological functions evolve during pedogenesis of loess-derived soil remains to be clarified.

In this research, we carried out a natural experiment by the careful selection of sites to create a sequence of loess-derived soils with varying degrees of pedogenic modification. One purpose of this study was to determine the pattern of co-variation of SOC and carbonate in loess-derived soil along an altitudinal gradient. In addition, several function-related soil properties, including soil pH, C/N ratio, CEC, bulk density and soil water retention at saturation (SWRs), field capacity (SWRf) and wilting point (SWRw), were investigated in relation to soil particle-size components, SOC and carbonate to obtain a better understanding of the evolutionary processes of loess-derived soil and the functioning of loess ecosystems.

Materials and methods

Study region

The Qilian Mountains form the northeast border of the Qinghai-Tibetan Plateau (Figure 1a). Their altitude decreases sharply from above 5500 m to less than 2000 m. At the regional scale, temperature and precipitation are controlled largely by altitude. Meteorological information from 10 weather stations at elevations from 4166 to 1483 m across the upper reach of the Heihe River was analysed by Chen *et al.* (2014); they found that the mean annual precipitation is closely related to altitude (about 200 mm at 1800 m, 600 mm at 3800 m), with an increasing gradient of about 200 mm km^{-1}. The mean annual temperature decreases at a rate of about 4.8°C km^{-1} (about 6.5°C at 1800 m, −3°C at 3800 m) (Table S1, Supporting Information). Other topographical elements such as aspect and slope shape could also modify local climate by affecting the reallocation of heat and water (Yang *et al.,* 2015). The landscape type is closely related to the heat–water combinations along the environmental gradient. Areas above 4000 m are mainly covered with ice or snow, and are cold desert zones with almost no vegetation. We sampled along a transect from 1849 to 3856 m. The landscape varies with increasing altitude from desert steppe in the arid foreland region (Figure 1b) to steppe or coniferous forest in the subalpine region (Figure 1d) and meadow or shrubby meadow in the alpine setting (Table 1).

Loess and loess-derived soil along the environmental gradient

Deposition of loess during the Holocene has been a regional phenomenon along the northern foreland of the Qilian Mountains and in some other upper mountainous regions (Kaiser *et al*., 2007; Yang *et al*., 2014, 2016; Nottebaum *et al*., 2015). Typically, soil on stable upper land in the Qilian Mountains has a surface soil horizon that is silty and has few stones, but below this there is a sharp change into clastic horizons that are composed mainly of fresh rock fragments (Figure 1e, Table 1). The contrast between silty surface horizons and underlying clastic layers is a typical feature of lithological discontinuity. This indicates that the soil layer in alpine and subalpine regions of this area is essentially derived from loess rather than from substrate rocks (Yang *et al*., 2016). Loess-like soil is pale yellow (Figure 1c) along the foreland region, whereas loess-derived alpine and subalpine soil is much darker in colour because of the larger SOC and water contents. In addition, the calcareous reaction decreases with the darkness of the soil. All soil samples have a silt loam texture and a Munsell hue of 7.5YR or 10YR (Table 1), which are typical of loess-derived soil. According to the World Reference Base (WRB) 2014 classification (IUSS Working Group WRB, 2014), the desert steppe soil is a Cambic Calcisol, whereas in subalpine and alpine settings the soil is more diverse and includes Cambic Calcisols, Chernic Phaeozems, Calcic Kastanozems, Calcic Chernozems, Skeletic Cambisols and Cryosols (Table 1).

Soil sampling

The design of this study was based on the assumption that the soil that was sampled has a uniform origin (i.e. Holocene loess), which previous sedimentological research, field soil morphology and particle-size distribution curves have shown to be the case (Küster *et al*., 2006; Nottebaum *et al*., 2014, 2015). To ensure the validity of this assumption, the soil morphology, including horizonation, particle-size classes, colour and calcareous reaction classes (Table 1), was examined carefully at all the sites proposed for purposive sampling. The sampling sites cover a wide range of areas, for example elevation ranges from 1848 to 3856 m. This is approximately the altitudinal zone for the distribution of loess surveyed by Nottebaum *et al.* (2014). The soil on moderate or gentle slopes was sampled to represent the soil of typical landscapes at each altitude. Twenty-three sites were selected and sampled.

Composite and core soil samples were taken separately at the same depth: 5–15-cm depth below ground surface. We deliberately excluded the top 5 cm because the topmost soil layer was likely

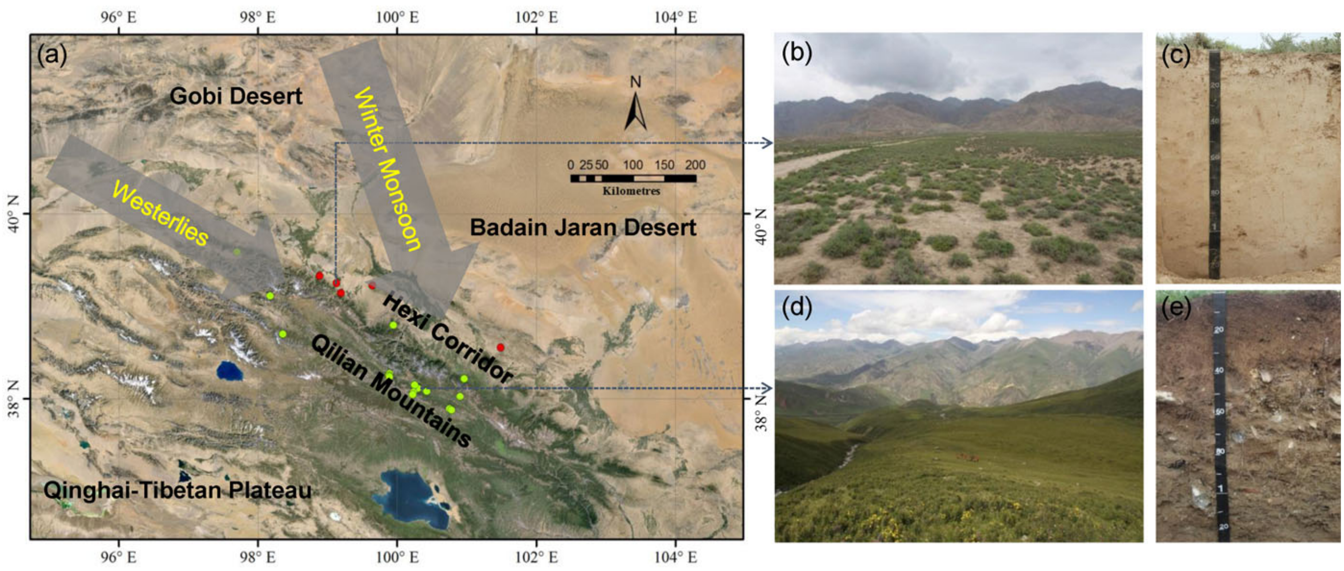

Figure 1 (a) The Qilian Mountains are on the northeast margin of the Qinghai-Tibetan Plateau and downwind of vast arid areas. Soil samples include five loess-like soils (red dots) along the arid foreland region and 18 loess-derived soils (green dots) in alpine and subalpine regions across the Qilian Mountains, (b) landscape and (c) soil profile of a representative site (site 3) in the arid foreland region, and (d) landscape and (e) soil profile of a representative site (site 12) in the subalpine region.

to have been affected by animal trampling in alpine settings and crusting in arid areas. Cores were taken in triplicate at each site and surrounding soil was also collected to form a composite soil sample.

Laboratory analysis

The composite soil samples were air-dried, fine roots were removed by hand, and the soil was sieved through a 2-mm sieve and then ground with an agate mortar. Soil particle-size distribution was analysed by a laser diffraction particle-size analyser (LS230, Beckman Coulter, Fullerton, CA, USA). Prior to the analysis, ~0.2 g of each soil sample was prepared by adding 30% H_2O_2 (hydrogen peroxide) and 5 mol l^{-1} HCl (hydrochloric acid) to remove organic matter and carbonate. Sodium hydroxide (NaOH) was used as the dispersant, and the sample solution was ultrasonicated for 10 minutes before measurement (Zhang & Gong, 2012). Soil mineralogy of the <2 mm fraction was determined with an X-ray diffractometer (Rigaku Ultima IV, Tokyo, Japan) after all samples were ground to pass through a 74-μm sieve. The relative abundance of minerals was quantified with the RockJock program (Eberl, 2003). The SOC content was determined by the wet oxidation method (Nelson & Sommers, 1982). Total nitrogen (TN) was measured by the Kjeldahl digestion procedure (Gallaher *et al*., 1976). The C/N ratio was calculated as the ratio of SOC to total nitrogen. Soil pH was measured in a 1:2.5 soil : water solution. Carbonate concentration (expressed as $CaCO_3$ equivalent) was determined by treating the sample with HCl and the CO_2 emitted was measured manometrically. The CEC was determined with NH_4OAc-EDTA as the extractant and buffered at pH 7 for acid or neutral soil and pH 8.5 for calcareous soil (Zhang & Gong, 2012). The CEC was re-measured after SOC had been removed by heating at 550°C for 4 hours. Soil cores were used to determine soil water retention and bulk density only. Soil water retention at saturation (SWRs) was measured as saturated soil water content by volume. Specifically, undisturbed soil samples in ring cores were saturated with water for 48 hours. During this process, the water level was gradually raised by adding water to 1 mm below the core's upper edge to exclude air entrapped in the soil. After weighing, saturated soil samples were transferred to a pressure plate apparatus to measure water contents at −33 and −1500 kPa to represent soil water retention at field capacity (SWRf) and wilting point (SWRw). Ten days and 28 days were needed to reach equilibrium for these two matric potentials, respectively. The cores were then oven dried at 105°C for 24 hours and weighed to calculate the bulk density.

Data analysis

The relations of altitude and soil properties with SOC and carbonate were determined by structural analysis, implemented in the R environment for statistical computing (R Core Team, 2016). Structural analysis of two variables determines the best-fitting line that expresses their relation, taking into consideration the error variances of the respective determinations (Webster, 1997). It is used in preference to regression when the aim is to determine a relation rather than to predict a response variable from a predictor variable. In structural analysis the error in the relation is not all assigned to the response variable as in linear regression, but rather is partitioned among the two variables whose relation is sought. To estimate structural relations, known precision from our laboratory was used for

Table 1 Altitude, landscape, soil type and field soil morphologies of the sampled sites

Site	Altitude / m	Landscape	Soil type (WRB)[a]	Lithological discontinuity[b]	Gravels / %[c]	Soil texture[d]	Munsell colour[e]	Calcareous reaction classes[f]
1	1849	Desert steppe	Cambic Calcisols	No	< 1	Silt loam	10YR 5/4	+++
2	2074	Desert steppe	Cambic Calcisols	No	< 1	Silt loam	10YR 5/3	+++
3	2177	Desert steppe	Cambic Calcisols	No	< 1	Silt loam	10YR 5/4	+++
4	2201	Desert steppe	Cambic Calcisols	No	< 1	Silt loam	10YR 4/4	+++
5	2331	Desert steppe	Cambic Calcisols	No	< 1	Silt loam	10YR 4/4	+++
6	2695	Subalpine steppe	Cambic Calcisols	No	< 1	Silt loam	10YR 4/4	++
7	2739	Subalpine steppe	Cambic Calcisols	No	< 1	Silt loam	10YR 3/4	+
8	2805	Subalpine steppe	Chernic Phaeozems	No	< 1	Silt loam	7.5YR 3/2	+
9	2973	Subalpine steppe	Calcic Kastanozems	No	< 1	Silt loam	7.5YR 4/3	−
10	2989	Coniferous forest	Chernic Phaeozems	No	< 1	Silt loam	10YR 2/3	−
11	3004	Coniferous forest	Chernic Phaeozems	No	< 1	Silt loam	7.5YR 2/2	−
12	3008	Subalpine steppe	Skeletic Cambisols	Yes	2	Silt loam	10YR 3/2	−
13	3119	Subalpine steppe	Cambic Calcisols	Yes	2	Silt loam	7.5YR 5/4	++
14	3129	Subalpine steppe	Calcic Chernozems	No	< 1	Silt loam	10YR 3/2	+
15	3152	Subalpine steppe	Skeletic Cambisols	Yes	< 1	Silt loam	10YR 2/3	−
16	3367	Subalpine steppe	Cambic Calcisols	Yes	2	Silt loam	10YR 3/3	+
17	3412	Alpine meadow	Calcic Chernozems	Yes	< 1	Silt loam	7.5YR 3/2	−
18	3539	Alpine meadow	Chernic Phaeozems	Yes	2	Silt loam	10YR 3/2	−
19	3573	Alpine meadow	Calcic Chernozems	Yes	< 1	Silt loam	10YR 3/3	+
20	3632	Shrubby meadow	Umbric Cryosols	Yes	2	Silt loam	7.5YR 3/2	−
21	3744	Shrubby meadow	Cambic Cryosols	Yes	5	Silt loam	10YR 3/3	−
22	3780	Alpine meadow	Mollic Cryosols	Yes	2	Silt loam	7.5YR 3/3	+
23	3856	Shrubby meadow	Skeletic Cryosols	Yes	10	Silt loam	7.5YR 3/3	−

[a]World Reference Base for Soil Resources (IUSS Working Group WRB, 2014).
[b]Lithological discontinuity represents zone of lithological change of soil parent material. We determined if lithological discontinuity exists in soil profiles within 1 m.
[c]Field soil morphologies, including gravel content, soil texture, soil colour and calcareous reaction classes were all described at 5–15-cm depth of the soil profile. Gravel content was estimated in the field by volume.
[d]This soil texture is estimated in the field by hand.
[e]Soil colour is recorded in moist condition with Munsell colour chart.
[f]Calcareous reaction classes describe reaction of soil matrix with 3 mol l^{-1} HCl. Specifically, +++ indicates strongly effervesces, ++ moderately effervesces, + slightly effervesces, − no effervescence.

the primary soil properties, the error variance of the C/N ratio was computed from the two primary variances by error propagation and the error variance of elevation was estimated from reported vertical precision of the Shuttle Radar Topography Mission data (Farr *et al*., 2007). Unless specified otherwise, the data represented results from the whole sample (23 sites). For the cores, the three replicates were used to estimate the mean value for further statistical analysis.

A principal component analysis (PCA) was carried out to identify the interrelations among all soil properties by CANOCO 4.5 (ter Braak & Šmilauer, 2002). The PCA was performed on the correlation matrix, which effectively standardizes the variables measured on different scales. Note that this PCA is based on a purposive sample, and therefore reflects the soil–landscape relations revealed by this representative sample. It is not intended as an unbiased estimate of correlations among these variables studied; rather it is an exploration of the relations in order to interpret pedogenesis in this landscape.

Results

Particle-size distribution and mineralogy

All soil samples had a silty loam texture (Figure S1, Supporting Information). Silt (2–50 μm) was the dominant fraction; it accounted for more than 60% of the composite samples (Table 2). Five loess-like soil samples (sites 1–5) from the desert steppe along the foreland region had the smallest clay content and showed little pedogenic modification because of the aridic soil moisture regime. Soil particle-size distribution was fairly uniform, with a peak value at ~35 μm in all soil samples (Figure S1, Supporting Information).

The mineral composition of all soil samples was dominated by quartz (52–69%). The most remarkable change in mineralogy was between the calcareous minerals (i.e. calcite and dolomite) (Figure 2). A substantial amount of calcite plus dolomite (14–22%) was present in the loess-like soil along the foreland region, whereas their contents were much smaller or even absent in the alpine or subalpine soil. Clay minerals for all soil samples were consistently dominated by illite (12–23%) and chlorite (7–15%).

Table 2 Physical and chemical soil properties of soil samples studied

Site	Clay / %	Silt / %	Sand / %	SOC / g kg^{-1}	TN / g kg^{-1}	C/N	CEC / cmol$_c$ kg^{-1}	$CaCO_3$ equivalent / g kg^{-1}	pH	BD / g cm^{-3}	SWRs / %	SWRf / %	SWRw / %
1	9	68	23	4	0.4	10.0	4.2	119	8.2	1.15 (0.07)[a]	55 (2.2)	36 (2.8)	20 (1.9)
2	9	72	19	6	0.6	10.0	5.1	173	8.5	1.22 (0.04)	53 (1.1)	35 (2.2)	18 (1.0)
3	9	72	19	5	0.5	10.0	4.2	166	8.4	1.25 (0.11)	49 (1.6)	30 (5.2)	14 (3.4)
4	10	72	18	7	0.7	10.0	4.9	152	8.7	1.20 (0.03)	54 (1.2)	33 (2.3)	17 (1.4)
5	11	70	19	12	1.3	9.2	7.2	78	8.5	1.21 (0.05)	50 (1.5)	30 (2.4)	15 (1.7)
6	12	72	16	19	2.0	9.5	7.7	127	8.2	1.13 (0.03)	52 (0.6)	35 (2.2)	16 (1.0)
7	12	76	12	27	2.9	9.3	12.3	49	8.4	0.91 (0.13)	57 (1.3)	32 (3.9)	15 (0.1)
8	12	69	19	46	4.6	10.0	27.6	9	8.0	0.96 (0.07)	63 (2.5)	40 (2.7)	27 (2.9)
9	12	63	25	33	3.5	9.4	21.7	7	7.8	1.03 (0.02)	53 (1.3)	38 (2.1)	19 (1.6)
10	14	73	13	118	7.5	15.7	60.5	8	7.0	0.45 (0.05)	75 (2.8)	41 (1.8)	25 (1.3)
11	17	68	15	111	6.5	17.1	54.4	13	6.6	0.36 (0.03)	74 (4.9)	42 (1.9)	30 (3.0)
12	13	62	25	53	4.5	11.8	30.6	5	7.9	0.81 (0.03)	60 (3.2)	35 (1.4)	20 (1.9)
13	13	71	16	25	2.6	9.6	9.2	114	8.3	1.02 (0.04)	55 (1.8)	35 (1.0)	23 (1.2)
14	12	63	25	45	4.2	10.7	28.3	13	8.1	0.68 (0.05)	64 (3.0)	31 (2.7)	15 (3.4)
15	13	62	25	65	5.3	12.3	38.6	3	7.5	0.53 (0.05)	72 (1.9)	40 (1.9)	27 (2.4)
16	15	69	16	38	3.6	10.6	18.2	50	8.2	0.91 (0.03)	60 (0.4)	34 (2.0)	21 (1.7)
17	14	72	14	50	4.2	11.9	31.1	7	7.7	0.87 (0.06)	63 (4.9)	38 (1.5)	25 (2.0)
18	13	69	18	66	5.2	12.7	36.0	1	6.5	0.73 (0.06)	64 (2.1)	37 (0.2)	26 (0.4)
19	13	71	16	43	3.9	11.0	22.2	24	8.2	0.66 (0.10)	67 (3.1)	32 (1.3)	17 (2.9)
20	16	64	20	46	4.0	11.5	24.8	2	6.8	0.92 (0.06)	59 (1.6)	36 (3.0)	23 (4.0)
21	12	66	22	65	5.5	11.8	31.7	6	6.7	0.83 (0.03)	56 (3.6)	38 (3.9)	24 (1.9)
22	13	66	21	83	6.6	12.6	36.2	17	7.7	0.85 (0.02)	66 (5.2)	35 (1.4)	24 (2.3)
23	17	75	8	79	5.9	13.4	33.9	10	7.1	0.63 (0.03)	72 (6.8)	41 (3.0)	30 (2.9)
Ref.[b]	9	68	23	4	0.4	10.0	4.0	174	8.4	–	–	–	–

[a]The data for BD, SWRs, SWRf and SWRw are mean values of the replicated samples and the standard deviations are given in parentheses.
[b]Ref. (reference soil) is taken from C horizon of site 2, which might be considered as the starting point of pedogenesis on loess.
SOC, soil organic carbon; TN, total nitrogen; C/N, ratio of soil organic carbon to total nitrogen; CEC, cation exchange capacity; BD, bulk density; SWRs, soil water retention at saturation; SWRf, soil water retention at field capacity; SWRw, soil water retention at wilting point.

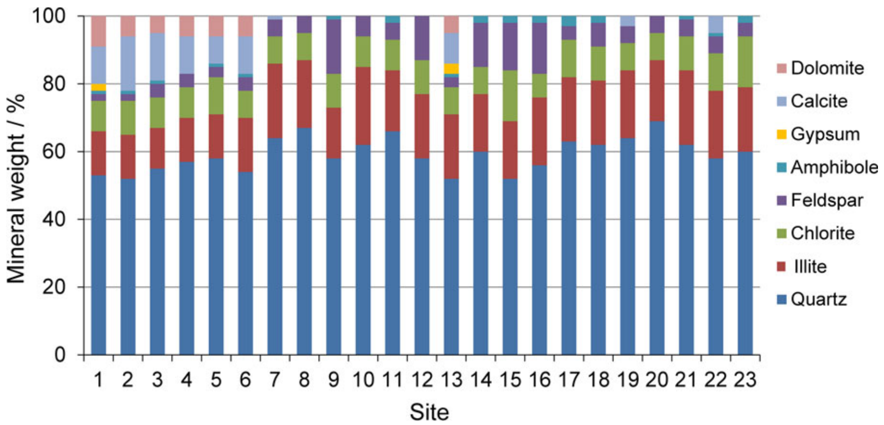

Figure 2 Quantitative mineralogy of the soil samples measured by X-ray diffraction and quantified by the RockJock program.

Soil organic carbon and carbonate

Soil organic carbon content varied from 4 to 118 g kg^{-1} and showed an increasing structural relation with altitude ($R^2 = 0.79$, excluding two forest sites) (Figure 3a). Two coniferous forest sites at ~3000 m had much larger SOC contents (>110 g kg^{-1}) than the soil at other sites. Five desert steppe sites with elevations below 2600 m had quite a small SOC content (average 7 g kg^{-1}). Calcium carbonate equivalent concentration, on the other hand, showed a decreasing structural relation with altitude ($R^2 = 0.58$) (Figure 3b). Calcium carbonate equivalent and SOC were inversely related before SOC accumulates to about 50 g kg^{-1} ($R^2 = 0.82$, $n = 16$). In this range (left side of the red dashed line in Figure 3c), $CaCO_3$ equivalent declined from 173 g kg^{-1} to less than 10 g kg^{-1}. However, carbonate was not exhausted because SOC continued to

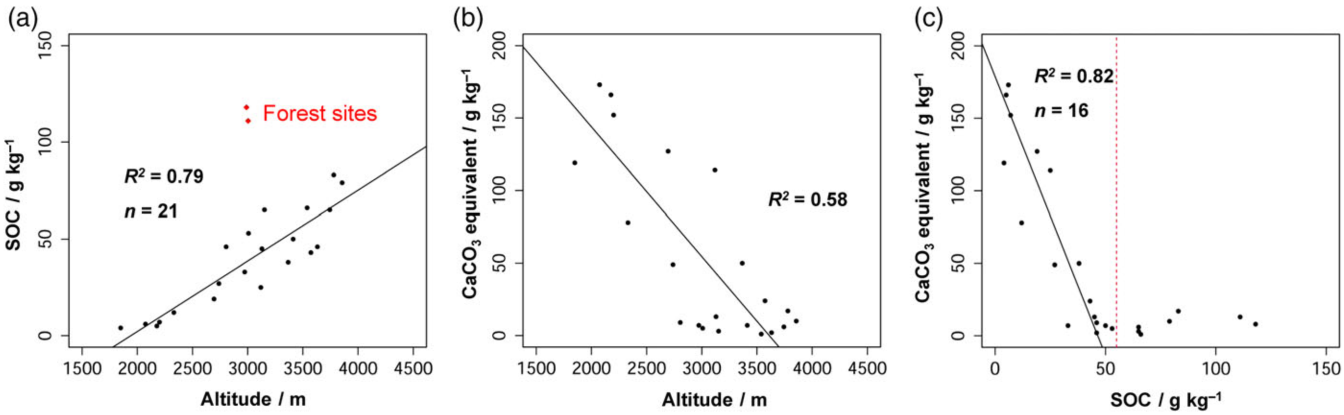

Figure 3 Variation in (a) soil organic carbon (SOC) and (b) $CaCO_3$ equivalent with altitude, and (c) relation between SOC and $CaCO_3$ equivalent. Two forest sites (marked as red diamonds) were excluded from the structural relation between altitude and SOC (a). The red dashed line in (c) separates the 16 samples to the left that were used in the structural analysis from the others.

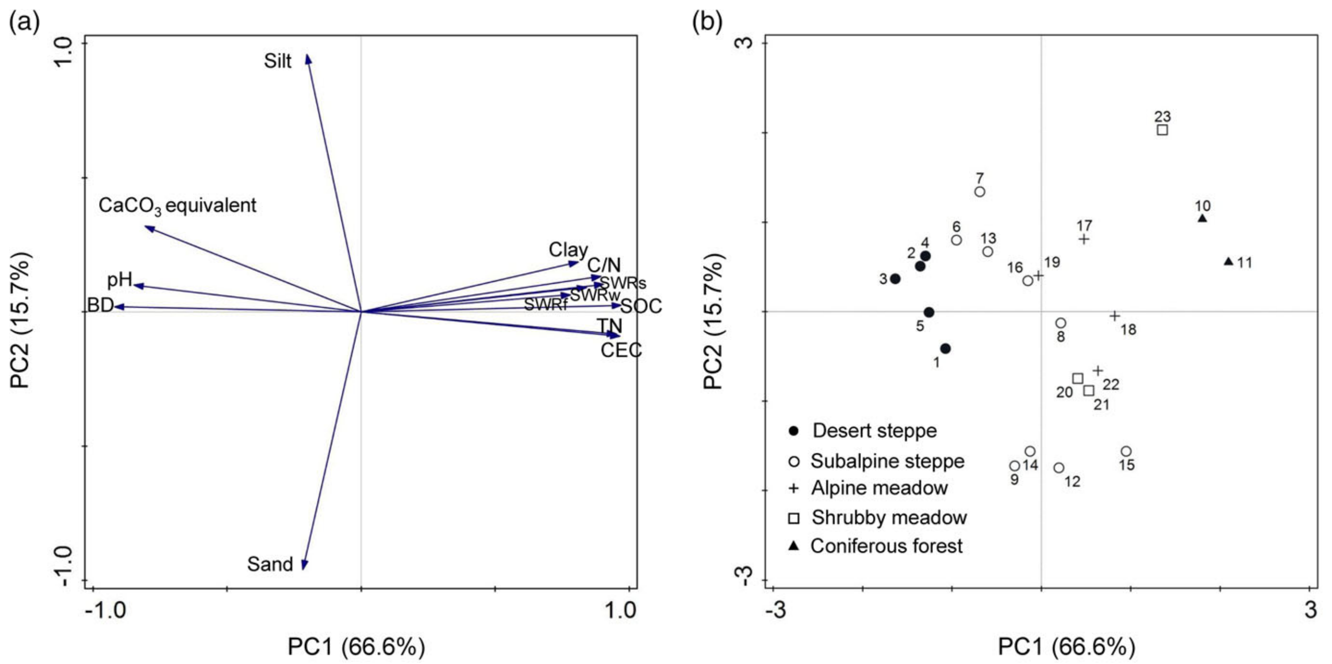

Figure 4 Principal component analysis (PCA): (a) eigenvector values of 13 variables plotted in the plane of the first two principal components and (b) PC scores of 23 soil samples plotted in the plane of the first two principal components. PC1 explains 66.6% of all variance and PC2 explains 15.7% of all variance.

increase, but fluctuated within the range of 1–17 g kg^{-1} $CaCO_3$ equivalent (right side of the red dashed line in Figure 3c).

Relations between soil carbon and other soil properties

The principal component analysis (PCA) provided a good summary of the variation in all the variables and samples (Figure 4). The first two principal components accounted for 82.3% of the total variance in the variables, with 66.6% of this for the first component (PC1). The first component (PC1) shows strong positive relations with SOC, TN, C/N ratio, CEC, clay content and soil water retention, and strong negative relations with $CaCO_3$ equivalent, pH and bulk density (Figure 4a). These two groups of variables account for a large proportion of the variation along PC1. All of these soil properties had eigenvector values greater than 0.75 (absolute value) on PC1. The second principal component (PC2) is primarily related to particle-size distribution with a strong negative relation between silt and sand; both have large eigenvector values along PC2. These two variables show no relation with the other soil properties on component 1 in the plane of the first two principal components. The plot of PC scores (Figure 4b) shows the relation between samples from different landscapes in the plane of the first two components. Desert steppe soil samples with the smallest SOC contents and largest $CaCO_3$ equivalent contents are clustered at the negative

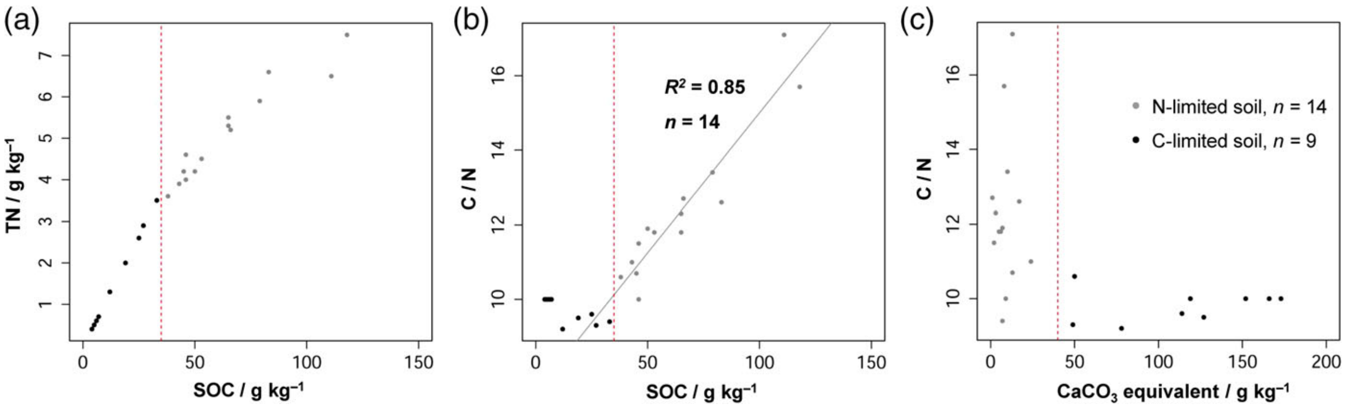

Figure 5 Variation in: (a) total nitrogen (TN) with soil organic carbon (SOC), (b) C/N in relation to SOC and (c) C/N in relation to $CaCO_3$ equivalent. The vertical red dashed line shows a threshold in SOC at ca. 35 g kg^{-1}.

extreme of PC1, whereas coniferous forest samples with the largest SOC contents are located on the positive extreme. Subalpine steppe, alpine meadow and shrubby meadow sites are mainly in the central area, showing continuous variation between the two extremes of coniferous forest and carbonate-rich samples. The subalpine steppe is closest to the desert steppe and the two meadow land uses are closest to the coniferous forest samples. To get some deeper insight into these patterns of variation among the variables and underlying processes, the correlations between soil carbon and individual soil properties were examined further.

The patterns of variation in TN and C/N with SOC show a threshold in SOC at ca. 35 g kg^{-1} (see vertical red dashed line in Figure 5). The rate of increase in TN with SOC decreases when SOC content exceeds this threshold, whereas below this TN increases linearly with SOC ($R^2 = 0.99$, $n = 9$) (Figure 5a). Correspondingly, the C/N ratio remains relatively constant at between 9.2 and 10.0 when SOC content is less than 35 g kg^{-1}. When SOC exceeds 35 g kg^{-1}, the C/N ratio increases from 10.0 to 17.1 with the increase in SOC ($R^2 = 0.85$, $n = 14$) (Figure 5b). Similarly, a threshold can be identified in the relation between C/N and $CaCO_3$ equivalent where $CaCO_3$ equivalent decreases between 24 and 50 g kg^{-1} (Figure 5c). The largest values of C/N were at the two forest sites.

Soil pH was relatively constant in the alkaline range (between pH 8.2 and 8.7) provided that the $CaCO_3$ equivalent concentration was more than 24 g kg^{-1}. However, it varied from pH 6.5 to 8.1 when $CaCO_3$ equivalent concentration was below 24 g kg^{-1} (Table 2). In addition, soil pH decreased with the increase in SOC ($R^2 = 0.64$).

The CEC increased linearly from 4.2 to 60.5 $cmol_c$ kg^{-1} with increasing SOC ($R^2 = 0.96$) (Figure 6). This effect was also reflected by the sharp decrease in CEC between 4.1 and 8.2 $cmol_c$ kg^{-1} when SOC was removed through burning. The small CEC of soil after the removal of SOC reflects the contribution from the mineral soil. Contributions of SOC to CEC varied from 2.4 to 88.1%.

Soil bulk density decreased from 1.25 to 0.36 g cm^{-3} with an increase in SOC ($R^2 = 0.81$) (Figure 7a). The accumulation of SOC enhanced SWRs from 49 to 75% ($R^2 = 0.77$) (Figure 7b), SWRf

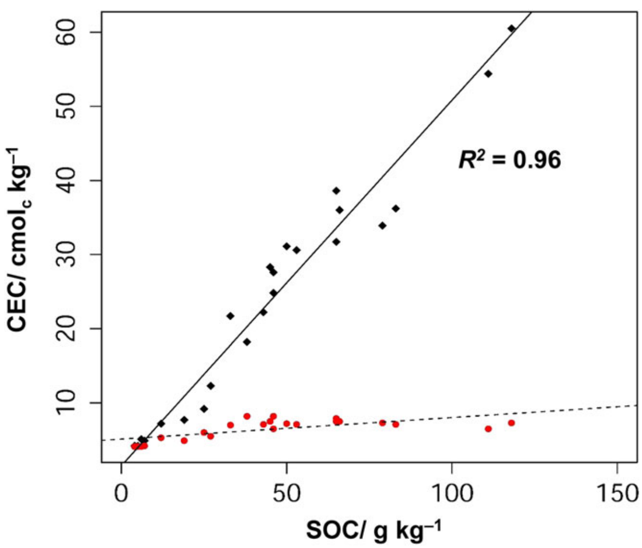

Figure 6 Relation between cation exchange capacity (CEC) and soil organic carbon (SOC). The black diamonds and the red dots are CEC contents for the same soil samples before and after combustion, respectively.

from 30 to 42% ($R^2 = 0.49$) (Figure 7c) and SWRw from 14 to 30% ($R^2 = 0.56$) (Figure 7d).

Discussion

Pedogenic modification from uniform loess to diverse soil types

Surface soil in the Qilian Mountains has a fairly uniform particle-size distribution and mineralogy (except for calcareous minerals), irrespective of the contrasting environmental conditions and different pedogenetic processes. This is attributed to the continuous deposition of loess sediments from the early Holocene to the present, which provides homogeneous fine earth as the major source of soil parent material (Lehmkuhl *et al*., 2014; Yang *et al*., 2016). In practice, particle-size distribution curves are often used as an effective indicator to determine whether sediments have

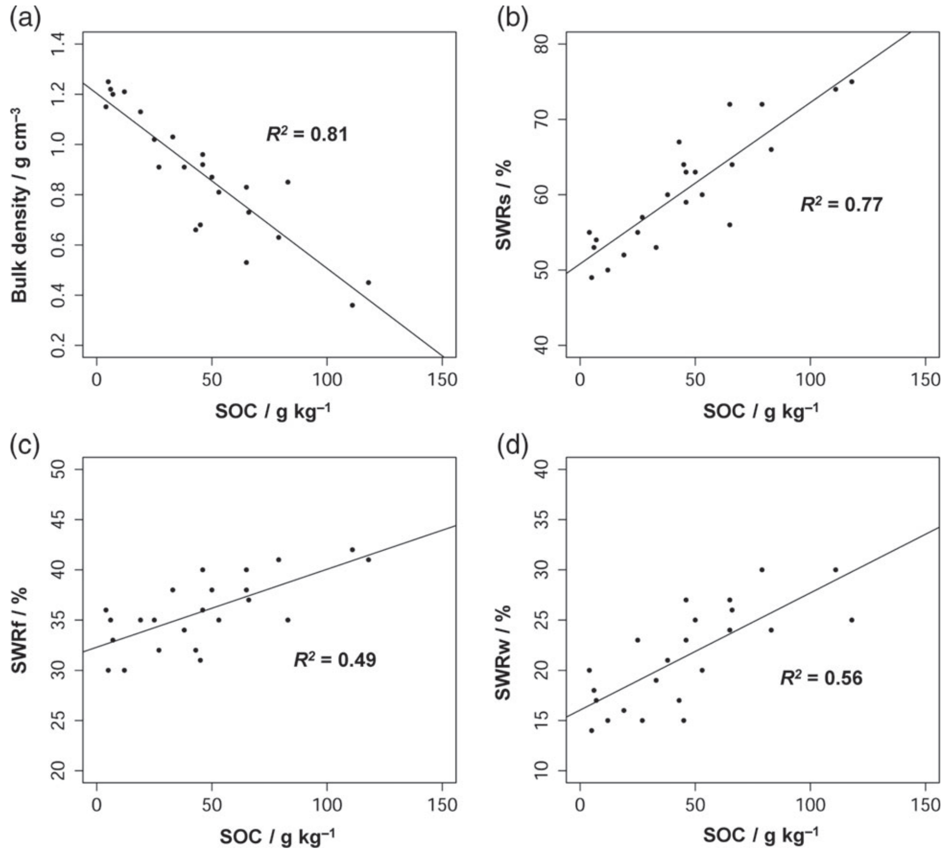

Figure 7 Relations between soil organic carbon (SOC) content and (a) bulk density, (b) soil water retention at saturation (SWRs), (c) field capacity (SWRf) and (d) wilting point (SWRw).

an aeolian origin (Vandenberghe, 2013; Yang *et al*., 2016). The consistent modal size at ~35 μm in all particle-size distribution curves suggests that alpine and subalpine soils share common sources of parent material with the loess at the northern foreland of the Qilian Mountains (Vandenberghe, 2013; Yang *et al*., 2016).

Chemical weathering of soil minerals is relatively weak because of the low temperatures in the high mountain region and the extreme aridity in the lower foreland region (precipitation/potential evapotranspiration <0.2 below 3000 m) (Bourque & Mir, 2012; Chen *et al*., 2014). This is evident from the persistent dominance of illite and chlorite in the clay fraction; these minerals are easily transformed into smectite or vermiculite in environments with greater weathering intensity (Egli *et al*., 2003). Leaching of carbonate appears to be the dominant chemical weathering process; calcite and dolomite are precursors in the chain of weathering of all soil minerals (Anderson *et al*., 2000). These calcareous minerals can be replenished by continuous additions of fresh loess sediments. Moreover, the leaching of carbonate is a prerequisite for several pedogenic processes, such as acidification and clay migration by illuviation (Chadwick & Chorover, 2001).

The coincident accumulation of SOC and leaching of carbonate along the environmental gradient are pedogenic responses to climatic forces. More water input and lower temperatures at higher altitudes favour the simultaneous accumulation of SOC and leaching of carbonate (Jenny, 1941). The leaching of carbonate depletes calcite and dolomite. The accumulation of SOC is essentially bound up with biological processes and is mainly controlled by soil moisture in this region (Liu *et al*., 2012). The production and decomposition of soil organic matter is in balance in arid regions where primary production and SOC accumulation are primarily limited by the scarcity of water (Wang *et al*., 2014). In alpine environments, however, the C/N ratio shows an increasing trend with SOC ($R^2 = 0.85$, $n = 14$), which suggests a decline in microbial activity in soil or poorer quality organic matter inputs (Post *et al.,* 1985; Vance & Chapin, 2001). The threshold patterns of variation in Figure 5 indicate a change from a C-limited loess ecosystem in arid regions to an N-limited one in alpine settings.

Strengthening of soil ecological functions

The accumulation of SOC and the leaching of carbonate trigger a series of changes in function-related soil properties. Soil pH is buffered in the alkaline pH range provided that carbonate is the dominant soil-acid-consuming component (Chadwick & Chorover, 2001). The H^+ generated by biological activity (e.g. production of CO_2 and organic acids) leads to the neutralization of soil pH,

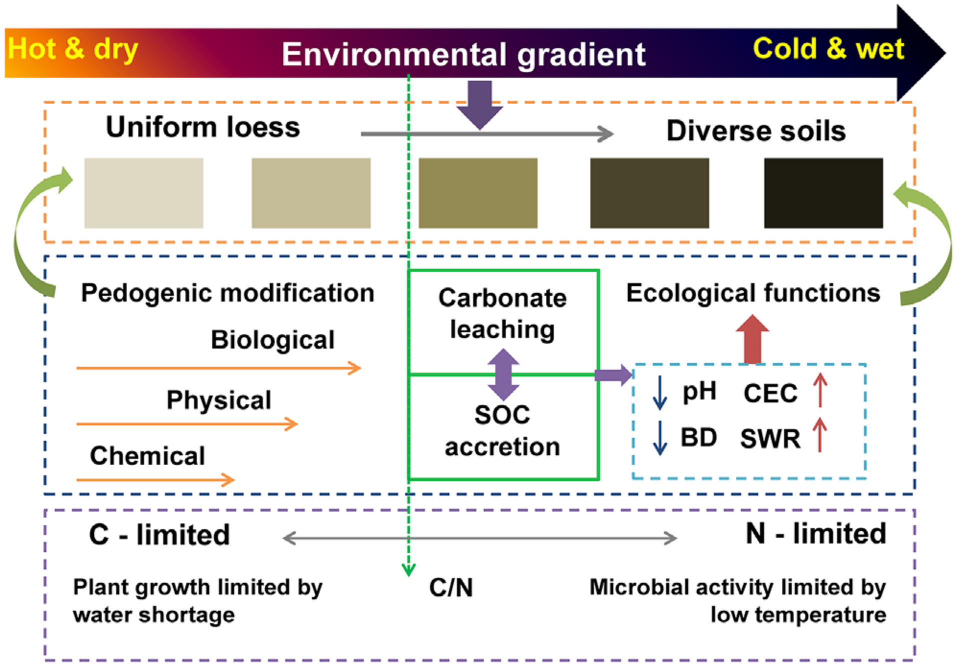

Figure 8 Conceptual diagram illustrating pedological and ecological implications of soil development on loess in response to the environmental gradient of the Qilian Mountains. BD, bulk density; CEC, cation exchange capacity; C/N, ratio of soil organic carbon to total nitrogen; SOC, soil organic carbon; SWR, soil water retention.

but only if the pH buffering system induced by CO_3^{2-}-HCO_3^- collapses after the exhaustion of carbonate. The near-neutral soil pH of the Qilian alpine ecosystem favours both microbial diversity and bioavailability of nutrients (Fierer & Jackson, 2006; Centeno & Alloway, 2013). The continuous addition of fresh loess materials precludes the acidification process, which is pronounced in many alpine ecosystems where a pH of < 3.5 is not uncommon (Körner, 2003).

The CEC is often used as an indicator of soil fertility or nutrient retention capacity (Schoenholtz *et al.*, 2000). In most cases, clay and SOC are two main contributors to CEC because they are the most important sources of negative charges in soil (Manrique *et al.*, 1991). In our case, however, the effect of clay on CEC is largely masked by SOC because of the larger variation in SOC than in clay. The enhancement of CEC depends on the accumulation of SOC in these loess-based ecosystems. This suggests that changes in SOC content might be linked to adsorption or the release of nutrient cations (e.g. K^+, Ca^+, Mg^+ and NH_4^+). In the case of intense forest or grass fire, the loss of SOC is largely responsible for the decrease in CEC and release of cations (Gimeno-García *et al.*, 2000). Although the temperature of forest or grass fires could be different from that of the furnace combustion of SOC in our research, the implication for the decrease in CEC from the loss of SOC is evident.

Soil bulk density is an index of many soil functions because it has a considerable effect on aeration, infiltration, water retention and biological processes (Meyer *et al.*, 2008; Yang *et al.*, 2014). Soil organic carbon effectively reduces soil bulk density and increases total porosity, which is related to SWRs (Figure 7). The negative correlation between soil bulk density and total porosity ($R^2 = 0.88$) indicates that SOC decreases bulk density of the loess sediments mainly by producing more pore spaces within the soil matrix. The enhancement of SWRf and SWRw might be because SOC promotes a large volume of meso- and micro-pores, which hold capillary and hygroscopic water, respectively (Farley *et al.*, 2004; Yang *et al.*, 2014).

Overall, as the uniform loess sediments evolve to diversify the soil across the environmental gradient studied, the accumulation of SOC and depletion of carbonate from arid to alpine environments are the two major pedogenic factors that modify the loess sediments, and at the same time they are responsible for the functional evolution of loess-derived soil (Figure 8). This, in turn, promotes biological activity and ecosystem functioning, which suggests that loess-derived soil might change in an evolutionary and self-enhancing way from arid to alpine settings.

Conclusions

With almost uniform parent material (i.e. Holocene loess) and contrasting ecosystems from arid to alpine, the loess-derived soil has evolved in different ways across the large environmental gradient. Soil particle-size distribution over this range is quite consistent because of the common origin of the soil material and the overall weak intensity of chemical weathering. Calcite and dolomite account for the major differences in soil mineralogy.

Accumulation of SOC and leaching of carbonate are the two major pedogenic factors in the modification of loess sediments.

Developments of some function-related soil properties are connected with the variation in SOC and carbonate during pedogenesis. Soil pH changes from alkaline in arid environments to near-neutral in alpine settings, which reflects the buffering by carbonate. The accretion of SOC effectively enhances CEC and SWR, showing that loess-derived soil with larger SOC content holds more nutrients and water. Also, soil porosity is enhanced, whereas bulk density is reduced by SOC. Thus, the accumulation of SOC and depletion of carbonate from arid to alpine environments dominate the functional evolution of loess-derived soil.

This research has also shown that climatic toposequences in loess provide potentially natural experiments to explore intrinsic soil behaviour together with the evolution of the whole ecosystem because the soil parent material is well defined. A good demonstration in our case is that variation in the C/N ratio shows threshold-like patterns with SOC and carbonate, which suggests a transition from C-limited arid environments to N-limited alpine regions with effects on the functioning of the ecosystem.

Supporting Information

The following supporting information is available in the online version of this article:

Table S1. Information on the sample sites (coordinates, altitude, local slope, MAT and MAP).

Figure S1. (a) Soil texture diagram (USDA) and (b) soil particle-size distribution curves of the soil samples studied. Five loess-like samples in the arid steppe are marked in red and the other soil samples are marked in blue.

Acknowledgements

We gratefully acknowledge the Editor-in-Chief, Professor Margaret A. Oliver, the Deputy Editor, Professor Edward M. Tipping, an anonymous Associate Editor, an anonymous referee and the statistics panel for their constructive comments. We also thank Decheng Li, Yuguo Zhao, Jinling Yang and Feng Liu (Institute of Soil Science, Chinese Academy of Sciences) for their help during the field work. This work was supported by the National Natural Science Foundation of China (Nos 41130530, 91325301 and 41571130051).

References

Anderson, S.P., Drever, J.I., Frost, C.D. & Holden, P. 2000. Chemical weathering in the foreland of a retreating glacier. *Geochimica et Cosmochimica Acta*, **64**, 1173–1189.

Bourque, C.P.A. & Mir, M.A. 2012. Seasonal snow cover in the Qilian Mountains of Northwest China: its dependence on oasis seasonal evolution and lowland production of water vapour. *Journal of Hydrology*, **454**, 141–151.

ter Braak, C.J. & Šmilauer, P. 2002. *CANOCO Reference Manual and CanoDraw for Windows User's Guide: Software for Canonical Community Ordination (Version 4.5)*. Microcomputer Power, Ithaca, NY.

Centeno, J.A. & Alloway, B.J. 2013. *Essentials of Medical Geology*. Springer, New York.

Chadwick, O.A. & Chorover, J. 2001. The chemistry of pedogenic thresholds. *Geoderma*, **100**, 321–353.

Chen, R.S., Liu, J.F., Kang, E.S., Yang, Y., Han, C.T., Liu, Z.W. *et al.* 2014. A cryosphere-hydrology observation system in a small alpine watershed in the Qilian Mountains of China and its meteorological gradient. *Arctic, Antarctic, & Alpine Research*, **46**, 505–523.

Eberl, D.D. 2003. *User Guide to RockJock-A Program for Determining Quantitative Mineralogy from X-ray Diffraction Data*. US Geological Survey, Washington.

Egli, M., Mirabella, A. & Fitze, P. 2003. Formation rates of smectites derived from two Holocene chronosequences in the Swiss Alps. *Geoderma*, **117**, 81–98.

Farley, K.A., Kelly, E.F. & Hofstede, R.G. 2004. Soil organic carbon and water retention after conversion of grasslands to pine plantations in the Ecuadorian Andes. *Ecosystems*, **7**, 729–739.

Farr, T.G., Rosen, P.A., Caro, E., Crippen, R., Duren, R., Hensley, S. *et al.* 2007. The shuttle radar topography mission. *Reviews of Geophysics*, **45**, RG2004.

Fierer, N. & Jackson, R.B. 2006. The diversity and biogeography of soil bacterial communities. *Proceedings of the National Academy of Sciences of the United States of America*, **103**, 626–631.

Gallaher, R.N., Weldon, C.O. & Boswell, F.C. 1976. A semiautomated procedure for total nitrogen in plant and soil samples. *Soil Science Society of America Journal*, **40**, 887–889.

Gimeno-García, E., Andreu, V. & Rubio, J.L. 2000. Changes in organic matter, nitrogen, phosphorus and cations in soil as a result of fire and water erosion in a Mediterranean landscape. *European Journal of Soil Science*, **51**, 201–210.

IUSS Working Group WRB. 2014. *World Reference Base for Soil Resources. International Soil Classification System for Naming Soils and Creating Legends for Soil Maps*. World Soil Resources Report No 106, FAO, Rome.

Jenny, H. 1941. *Factors of Soil Formation: A System of Quantitative Pedology*. McGraw-Hill, New York.

Kaiser, K., Schoch, W.H. & Miehe, G. 2007. Holocene paleosols and colluvial sediments in Northeast Tibet (Qinghai Province, China): properties, dating and paleoenvironmental implications. *Catena*, **69**, 91–102.

Klopfenstein, S.T., Hirmas, D.R. & Johnson, W.C. 2015. Relationships between soil organic carbon and precipitation along a climosequence in loess-derived soils of the Central Great Plains, USA. *Catena*, **133**, 25–34.

Körner, C. 2003. *Alpine Plant Life: Functional Plant Ecology of High Mountain Ecosystems*. Springer–Verlag, Heidelberg.

Küster, Y., Hetzel, R., Krbetschek, M. & Tao, M. 2006. Holocene loess sedimentation along the Qilian Shan (China): significance for understanding the processes and timing of loess deposition. *Quaternary Science Reviews*, **25**, 114–125.

Lehmkuhl, F., Schulte, P., Zhao, H., Hülle, D., Protze, J. & Stauch, G. 2014. Timing and spatial distribution of loess and loess-like sediments in the mountain areas of the northeastern Tibetan Plateau. *Catena*, **117**, 23–33.

Liu, T.S. 1985. *Loess and the Environment*. China Ocean Press (in Chinese), Beijing.

Liu, W., Chen, S.Y., Qin, X., Baumann, F., Scholten, T., Zhou, Z.Y. *et al.* 2012. Storage, patterns, and control of soil organic carbon and nitrogen in the northeastern margin of the Qinghai–Tibetan Plateau. *Environmental Research Letters*, **7**, 035401.

Manrique, L.A., Jones, C.A. & Dyke, P.T. 1991. Predicting cation-exchange capacity from soil physical and chemical properties. *Soil Science Society of America Journal*, **55**, 787–794.

Meyer, C.K., Baer, S.G. & Whiles, M.R. 2008. Ecosystem recovery across a chronosequence of restored wetlands in the Platte River Valley. *Ecosystems*, **11**, 193–208.

Nelson, D.W. & Sommers, L.E. 1982. Total carbon, organic carbon and organic matter. In: *Methods of Soil Analysis, Part 2. Chemical and Microbiological Properties*, 2nd edn (ed. A.L. Page), pp. 539–579. ASA and SSSA, Madison, WI.

Nottebaum, V., Lehmkuhl, F., Stauch, G., Hartmann, K., Wünnemann, B., Schimpf, S. *et al.* 2014. Regional grain size variations in aeolian sediments along the transition between Tibetan highlands and north-western Chinese deserts–the influence of geomorphological settings on aeolian transport pathways. *Earth Surface Processes & Landforms*, **39**, 1960–1978.

Nottebaum, V., Stauch, G., Hartmann, K., Zhang, J. & Lehmkuhl, F. 2015. Unmixed loess grain size populations along the northern Qilian Shan (China): relationships between geomorphologic, sedimentologic and climatic controls. *Quaternary International*, **372**, 151–166.

Post, W.M., Pastor, J., Zinke, P.J. & Stangenberger, A.G. 1985. Global patterns of soil nitrogen storage. *Nature*, **317**, 613–616.

R Core Team 2016. *R: A Language and Environment for Statistical Computing*. Foundation for Statistical Computing, Vienna.

Schaetzl, R.J. & Anderson, S. 2005. *Soils: Genesis and Geomorphology*. Cambridge University Press, New York.

Schoenholtz, S.H., Van Miegroet, H. & Burger, J.A. 2000. A review of chemical and physical properties as indicators of forest soil quality: challenges and opportunities. *Forest Ecology & Management*, **138**, 335–356.

Vance, E.D. & Chapin, F.S. III 2001. Substrate limitations to microbial activity in taiga forest floors. *Soil Biology & Biochemistry*, **33**, 173–188.

Vandenberghe, J. 2013. Grain size of fine-grained windblown sediment: a powerful proxy for process identification. *Earth-Science Reviews*, **121**, 18–30.

Walker, D.A. & Everett, K.R. 1991. Loess ecosystems of northern Alaska: regional gradient and toposequence at Prudhoe Bay. *Ecological Monographs*, **61**, 437–464.

Wang, C., Wang, X.B., Liu, D.W., Wu, H.H., Lü, X.T., Fang, Y.T. *et al.* 2014. Aridity threshold in controlling ecosystem nitrogen cycling in arid and semi-arid grasslands. *Nature Communications*, **5**, 4799.

Webster, R. 1997. Regression and functional relations. *European Journal of Soil Science*, **48**, 557–566.

Yang, F., Zhang, G.L., Yang, J.L., Li, D.C., Zhao, Y.G., Liu, F. *et al.* 2014. Organic matter controls of soil water retention in an alpine grassland and its significance for hydrological processes. *Journal of Hydrology*, **519**, 3086–3093.

Yang, F., Huang, L.M., Li, D.C., Yang, F., Yang, R.M., Zhao, Y.G. *et al.* 2015. Vertical distributions of soil organic and inorganic carbon and their controls along toposequences in an alpine region. *Acta Pedologica Sinica*, **52**, 1226–1236 (in Chinese).

Yang, F., Zhang, G.L., Yang, F. & Yang, R.M. 2016. Pedogenetic interpretations of particle-size distribution curves for an alpine environment. *Geoderma*, **282**, 9–15.

Zhang, G.L. & Gong, Z.T. 2012. *Soil Survey Laboratory Methods*. Science Press (in Chinese), Beijing.